HHS Public Access

Author manuscript

Nat Commun. Author manuscript; available in PMC 2015 September 02.

Published in final edited form as:

Nat Commun. ; 5: 4691. doi:10.1038/ncomms5691.

Loss of PIKfyve in platelets causes a lysosomal disease leading to inflammation and thrombosis in mice

Sang H. Min[1], **Aae Suzuki**[1], **Timothy J. Stalker**[1], **Liang Zhao**[1], **Yuhuan Wang**[4], **Chris McKennan**[5], **Matthew J. Riese**[1], **Jessica F. Guzman**[1], **Suhong Zhang**[3], **Lurong Lian**[1], **Rohan Joshi**[1], **Ronghua Meng**[2], **Steven H. Seeholzer**[5], **John K. Choi**[6], **Gary Koretzky**[1], **Michael S. Marks**[2], and **Charles S. Abrams**[1]

[1]Department of Medicine, at the University of Pennsylvania School of Medicine, Philadelphia, PA 19104, USA

[2]Department of Pathology, at the University of Pennsylvania School of Medicine, Philadelphia, PA 19104, USA

[3]Department of Pharmacology, at the University of Pennsylvania School of Medicine, Philadelphia, PA 19104, USA

[4]Division of Hematology, St. Jude Children's Research Hospital, Memphis, TN, USA

[5]Proteomics core at The Children's Hospital of Philadelphia, St. Jude Children's Research Hospital, Memphis, TN, USA

[6]Hematopathology, St. Jude Children's Research Hospital, Memphis, TN, USA

Abstract

PIKfyve is a lipid kinase that is essential for the synthesis of phosphatidylinositol-3,5-bisphosphate [PtdIns(3,5)P_2], and for the regulation of membrane dynamics within the endolysosomal system in mammals. Depletion of intracellular pools of PtdIns(3,5)P_2 in humans and in mice is associated with neurodegeneration and early lethality. However, the biological role of PtdIns(3,5)P_2 in non-neural tissues is not well understood. Platelets are hematopoietic cells that function in a variety of physiological responses. Essential to many of these functions is the activation-dependent release of effectors from distinct storage granules - alpha granules, dense granules, and lysosomes - that derive from the endolysosomal system. Here we show that platelet-specific ablation of the PIKfyve gene in mice results in accelerated arterial thrombosis, but also unexpectedly to multiorgan defects that impair development, body mass, fertility, and survival by inducing inappropriate inflammatory responses characterized by macrophage accumulation in multiple tissues. Platelet depletion *in vivo* significantly impairs the progression of multiorgan defects in these mice, confirming that these defects reflect a platelet-specific process. Although

Correspondence should be sent to Charles S. Abrams, 421 Curie Blvd, Biomedical Research Bldg. II/III #812, Philadelphia, PA 19104, USA, Tel: 215-573-3288, abrams@mail.med.upenn.edu.

Author Contributions S.H.M planned and performed experiments, data analysis and presentation of most of the experiments, and wrote the manuscript; A.S. and T.J.S. carried out experiments; L.Z., Y.W., M.J.R., J. F. G., S.Z., L.L. and R.M. provided technical assistance; CM., and S.H.S., performed the proteomics experiments and analysis; J.K.C. contributed to the data analyses; G.A.K. and M.S.M. provided critical reagents and contributed to the data analyses; C.S.A. supervised the project and wrote the manuscript.

Author information The authors declare no competing financial interests.

PIKfyve-null platelets generate and release normal amounts of alpha granule and dense granule contents, they develop defective maturation and excessive storage of lysosomal enzymes, which are released upon platelet activation. Remarkably, impairing the secretion of lysosomes from PIKfyve-deficient platelets *in vivo* significantly attenuates the multiorgan defects in mice, suggesting that platelet lysosome secretion contributes to pathogenesis. Together, these results demonstrate that PIKfyve is an essential regulator for the biogenesis of platelet lysosomes, and highlight the previously unrecognized and important pathological contributions of platelet lysosomes in inflammation, arterial thrombosis, and macrophage biology.

Introduction

Phosphoinositides are minor components of membrane phospholipids, yet they are essential for the regulation of diverse cellular processes, including signal transduction, cytoskeletal control, and membrane trafficking[1]. Phosphoinositide metabolism is tightly modulated by specific lipid kinases and phosphatases. Altering phosphoinositide turnover by dysregulating these enzymes can lead to a variety of human diseases[2].

PtdIns(3,5)P_2 is a phosphoinositide of low abundance that is synthesized from PtdIns(3)P on the endosomal compartments in mammalian cells by the lipid kinase PIKfyve (also known as FAB1)[3]. PIKfyve forms a protein complex with other regulatory proteins, such as with the PtdIns(3,5)P_2 5-phosphatase Fig4 (also known as SAC3)[4,5] and the docking protein Vac14 (also known as ArPIKfyve)[6,7]. The PIKfyve complex and its product PtdIns(3,5)P_2 are essential regulators of membrane homeostasis, and of vesicle trafficking and cargo transport along the endosomal-lysosomal pathway[8,9] .

Recently, physiological functions of PtdIns(3,5)P_2 have been elucidated using genetically engineered mice that lack different components of the PIKfyve complex[10]. PIKfyve-null mice are embryonically lethal[11], but mice expressing residual PIKfyve activity are viable and develop defects within multiple organs, such as in the nervous, cardiopulmonary, and hematopoietic systems[12]. Similarly, Fig4-null mice or Vac14-null mice develop several defects, including neurodegeneration, hypopigmentation, and early lethality[13,14]. Notably, homozygous Fig4 mutations were also identified in patients who have the neurodegenerative diseases Charcot-Marie Tooth Syndrome 4J and Amyotrophic Lateral Sclerosis[14,15], demonstrating a role for PtdIns(3,5)P_2 in neural development. Although studies showed that PtdIns(3,5)P_2 deficiency causes defects in multiple cellular pathways including those required for endolysosomal trafficking in yeast and mammalian cell cultures, the physiological consequences of PtdIns(3,5)P_2 in non-neural cells, such as those of the hematopoietic system, is not well understood.

Platelets are hematopoietic cells that are crucial for hemostatic plug formation in response to vascular injury. This process has been shown to require a series of key platelet activation events that are tightly regulated by several phosphoinositides[16]. However, the regulatory role of PtdIns(3,5)P_2 in platelets remains unknown. Platelets are anucleated, but they store numerous biologically active substances in their secretory organelles, which include alpha granules, dense granules, and lysosomes[17,18]. Platelet granules are generated in

megakaryocytes from the endosomal-lysosomal system[19–22] by as yet, poorly understood mechanisms.

In this study, we investigated whether PIKfyve plays an essential role in platelets and in megakaryocytes using mice lacking PIKfyve specifically in these cell types. Given the role of PIKfyve-mediated PtdIns(3,5)P_2 production in the regulation of the endosomal-lysosomal pathway, we hypothesized that PIKfyve was essential for the biogenesis and function of platelet granules. We show that PIKfyve is critical for proper lysosomal homeostasis in platelets, but it is not necessary for the biogenesis of alpha granules or dense granules. Remarkably, PIKfyve-null platelets are defective in the maturation, storage, and release of lysosomal enzymes. Unexpectedly, these platelet lysosomal defects induce aberrant inflammatory responses in macrophages that impair the development, body mass, fertility, and survival of mice.

Results

Platelet-specific loss of PIKfyve in mice results in multiorgan defects

To investigate the role of PIKfyve in platelets and in megakaryocytes, we generated mice lacking PIKfyve kinase activity specifically in these cell types. The PIKfyve gene was conditionally targeted with loxP sites flanking the exons corresponding to the kinase activation loop to generate floxed alleles of PIKfyve (PIKfyve^{fl}, Fig. 1a). Mice expressing PIKfyve^{fl} were crossed with transgenic mice expressing the Cre recombinase that is controlled by the platelet-factor-4 promoter (Pf4-Cre), which restricts the expression of Cre recombinase exclusively within megakaryocytes and their derived platelets[23].

PIKfyve$^{fl/fl}$ Pf4-Cre mice developed several morphological abnormalities relative to their littermate PIKfyve$^{fl/+}$ mice, PIKfyve$^{fl/fl}$ mice, and PIKfyve$^{fl/+}$ Pf4-Cre mice. At about 3 weeks of age, PIKfyve$^{fl/fl}$ Pf4-Cre mice exhibited mild growth delay and body hair loss (Supplementary Fig. 1a). Over time, they gradually developed coarse facial features, abdominal distention, a generalized increase in the bulk of their soft tissues, and body weight gain (Fig. 1b and 1c). Despite this weight gain, body composition analysis by dual-energy X-ray absorptiometry showed that PIKfyve$^{fl/fl}$ Pf4-Cre mice had reduced body fat, but increased lean body mass, as compared to their littermate controls (Fig. 1d). In addition, they also had decreased bone mineral density (Supplementary Fig. 1b). As PIKfyve$^{fl/fl}$ Pf4-Cre mice aged, they remained infertile (Supplementary Fig. 1c) and their general body functions deteriorated. The vast majority died before 28 weeks of age (Fig. 1e).

Large vacuolated macrophages accumulate in multiple organs of PIKfyve$^{fl/fl}$ Pf4-Cre mice

To elucidate the cause of multiorgan defects in PIKfyve$^{fl/fl}$ Pf4-Cre mice, histological and immunohistochemical analyses were performed in mice of 3–28 weeks of age. Unlike their control littermates, PIKfyve$^{fl/fl}$ Pf4-Cre mice exhibited massive organomegaly (Supplementary Fig. 2a). This phenotype reflected progressive tissue infiltration by engorged cells with multiple cytoplasmic vacuoles that had a “foamy” appearance (Fig. 2a and Supplementary Fig. 2b, arrowheads). Although the vacuoles of these cells did not stain with classical dyes for proteins or lipids, their cytoplasm strongly stained with Alcian Blue

and PAS, suggesting an excessive storage of acidic polysaccharides in the vacuolated cells (Fig. 2b and Supplementary Fig. 3a). In their livers and lungs, the vacuolated cells accumulated in a perivascular distribution and displaced the normal tissue (Fig. 2a), suggesting that the vacuolated cells originated from the blood or vasculature. By immunohistochemical analysis, the vacuolated cells stained with the macrophage-specific marker F4/80 (Fig. 2c), but not with the markers of other cell lineages, including GPIb (a megakaryocyte-specific marker; data not shown). The F4/80-positive vacuolated macrophages in the livers of PIKfyve$^{fl/fl}$ Pf4-Cre mice were approximately 3–4 fold larger than the F4/80-positive macrophages in the livers of the control mice (Fig. 2d). In addition, tissues infiltrated with the vacuolated macrophages were often associated with mononuclear cell infiltrates that stained with the lymphocyte marker CD45R (Supplementary Fig. 3b), suggesting a local inflammatory response. These results demonstrate that the loss of PIKfyve in platelets causes the invasion of normal tissues with inflammatory vacuolated macrophages.

PIKfyve ablation in platelets induces non-autonomous defects in macrophages

PtdIns(3,5)P_2-deficient organisms have been shown to form large cytoplasmic vacuoles[9,10]. However, because our genetic approach was designed to only ablate PtdIns(3,5)P_2 synthesis in platelets and in megakaryocytes, we did not expect to see the robust cytoplasmic vacuolation in the macrophages of PIKfyve$^{fl/fl}$ Pf4-Cre mice. Therefore, we further addressed whether these unexpected macrophage abnormalities resulted from aberrant PIKfyve disruption in macrophages, or by non-autonomous effects of PIKfyve disruption in platelets. Immunoblotting analysis showed that PIKfyve protein was absent in platelets, but present in the liver, spleen, and lungs of PIKfyve$^{fl/fl}$ Pf4-Cre mice. PIKfyve protein was also present in all tissues of the control mice (Fig. 3a and Supplementary Fig. 4a). These results strongly suggest that the PIKfyve protein was ablated only in the megakaryocyte lineage of PIKfyve$^{fl/fl}$ Pf4-Cre mice.

Although Pf4-Cre expression has been shown to be restricted to megakaryocytes and platelets[23–26], we next re-evaluated Pf4-Cre expression in PIKfyve$^{fl/fl}$ Pf4-Cre mice by crossing them to mice expressing a Cre-dependent LacZ reporter (*Rosa26-LacZ*)[27]. Tissue staining of PIKfyve$^{fl/fl}$ Pf4-Cre/ *Rosa26-Lacz* mice with X-gal showed β-galactosidase expression only in megakaryocytes and in platelets (Fig. 3b and Supplementary Fig. 4b, arrows), but not in the vacuolated macrophages or in other cells (Fig. 3b, arrowheads). This genetic evidence excludes the possibility that Pf4-Cre induced PIKfyve ablation in the macrophages of PIKfyve$^{fl/fl}$ Pf4-Cre mice. Together, these results demonstrate that the macrophage infiltration and enlargement observed in PIKfyve$^{fl/fl}$ Pf4-Cre mice are indirectly induced by PIKfyve ablation in megakaryocytes and/or in platelets.

Platelet depletion attenuates the progression of the pathology in PIKfyve$^{fl/fl}$ Pf4-Cre mice

To further address whether PIKfyve-null platelets contribute to the robust macrophage response leading to the multiorgan failure in PIKfyve$^{fl/fl}$ Pf4-Cre mice, we studied the effects of platelet depletion using monoclonal GP1bα antibodies[28,29]. Platelet depletion was initiated at 8–10 weeks of age. At that point, the PIKfyve$^{fl/fl}$ Pf4-Cre mice had already developed body hair loss, some weight gain, and tissue infiltration of their vacuolated

macrophages. Control mice and PIKfyve$^{fl/fl}$ Pf4-Cre mice were either untreated or administered GP1bα antibodies twice weekly via intraperitoneal injections for 6 weeks. As reported previously, the injection of GP1bα antibodies efficiently induced acute thrombocytopenia in both sets of mice[28,29]. However, repetitive injections of GP1bα antibodies were less effective at inducing stable thrombocytopenia over time (data not shown). Nevertheless, the PIKfyve$^{fl/fl}$ Pf4-Cre mice that were treated with GP1bα antibodies showed a significant delay in weight gain and attenuated hair loss as compared to the untreated PIKfyve$^{fl/fl}$ Pf4-Cre mice (Fig. 3c and 3d). Together, our findings demonstrate that platelets are the primary contributors in the development of the inflammatory macrophage response and multiorgan defects in PIKfyve$^{fl/fl}$ Pf4-Cre mice.

We also investigated whether the macrophage response in PIKfyve$^{fl/fl}$ Pf4-Cre mice could be rescued or transferred by hematopoietic stem cell (HSC) transplantation. Lethally irradiated wild-type mice of 8–12 weeks of age were reconstituted with a mixture of donor cells that were half derived from PIKfyve$^{fl/fl}$ Pf4-Cre HSCs and half derived from wild-type HSCs. Thirty-five weeks later, a necropsy showed that infiltration of vacuolated macrophages was readily apparent in the liver, lung, colon, and bone marrow of the irradiated wild-type recipient mice (Supplementary Fig. 5b and 5e, arrowheads). Conversely, lethally irradiated PIKfyve$^{fl/fl}$ Pf4-Cre mice of 8–12 weeks of age were reconstituted exclusively with wild-type donor HSCs. At about 8 weeks after transplantation, the characteristic hair loss and weight gain were significantly attenuated. A necropsy at 35 weeks after transplantation confirmed that the infiltration of the vacuolated macrophages in multiple tissues was completely reversed (Supplementary Fig. 5c and 5f). Together, these results further demonstrate that the phenotype of PIKfyve$^{fl/fl}$ Pf4-Cre mice can be either rescued or transferred by hematopoietic progenitor cells.

Abnormal megakaryocyte morphology but normal megakaryocyte development and platelet production in the absence of PIKfyve

We next studied the effects of PIKfyve ablation in megakaryocytes of PIKfyve$^{fl/fl}$ Pf4-Cre mice. Fibroblasts and neurons of PtdIns(3,5)P_2-deficient organisms typically develop large vacuoles[9,10]. Histological analysis by light microscopy of bone marrow sections showed that PIKfyve-null megakaryocytes were morphologically indistinguishable from control megakaryocytes (data not shown). However, analysis by transmission electron microscopy of cultured megakaryocytes derived from PIKfyve$^{fl/fl}$ Pf4-Cre bone marrow revealed multiple enlarged cytoplasmic vacuoles (Fig. 4a). Despite this abnormality, flow cytometric analysis showed no significant differences in the number of megakaryocytes in the bone marrow of control or PIKfyve$^{fl/fl}$ Pf4-Cre mice (Fig. 4b). Moreover, PIKfyve-null megakaryocytes had normal ploidy, implying that the loss of PIKfyve did not affect megakaryocyte maturation (Fig. 4c). Finally, counts of platelets and leukocytes as well as hemoglobin level were similar between control and PIKfyve$^{fl/fl}$ Pf4-Cre mice (Fig. 4d, 4e and 4f). Thus, PIKfyve$^{fl/fl}$ Pf4-Cre mice normally develop megakaryocytes *in vivo* and produce normal numbers of platelets, and they also normally develop other blood cells.

Abnormal maturation, storage, and release of lysosomal components in PIKfyve-null platelets

We next investigated the effects of PIKfyve ablation in the morphology and functions of platelets in PIKfyve$^{fl/fl}$ Pf4-Cre mice. Transmission electron microscopy demonstrated that in contrast to the PIKfyve-null megakaryocytes derived from the bone marrow, the ultrastructure of PIKfyve-null platelets was indistinguishable from that of control platelets (Supplementary Fig. 6a). To test whether the loss of PIKfyve impacted granule content, we assessed the abundance of representative components by immunoblotting. PIKfyve-null platelets expressed normal levels of the alpha granule components von Willebrand factor and platelet factor 4 (Supplementary Fig. 6b and 6c). In contrast, PIKfyve-null platelets exhibited increased levels of the lysosomal protein LAMP-1 (Lysosomal-Associated Membrane Protein 1) (Fig. 5a) and increased activity of the lysosomal enzyme β-hexosaminidase (Fig. 5b). These results suggest that PIKfyve-null platelets store normal levels of alpha granule components, but store excessive levels of lysosomal components.

To test whether PIKfyve regulates granule secretion, we stimulated platelets *ex vivo* and monitored granule release by surface expression of granule markers or release of mediators into the medium. Following thrombin stimulation, PIKfyve-null platelets translocated the α-granule protein P-selectin to their cell surface as efficiently as control platelets (Supplementary Fig. 6d). Likewise, ATP secretion from dense granules was similar in control and PIKfyve-null platelets (data not shown). However, the releasates from PIKfyve-null platelets showed increased activity of the lysosomal enzyme, β-hexosaminidase (Fig. 5c). Further analysis showed that the PIKfyve-null platelets released a normal percentage of their total cellular β-hexosaminidase following agonist stimulation (Supplementary Fig. 7a). These data indicate that PIKfyve-null platelets release higher levels of β-hexosaminidase than the control platelets because they contain excessive amounts of this lysosomal enzyme, and not because they secrete it more efficiently. Consistent with this finding, β-hexosaminidase activity was found to also be elevated in the plasma of PIKfyve$^{fl/fl}$ Pf4-Cre mice (Fig. 5c). Together, these findings demonstrate that PIKfyve-null platelets store and release excessive levels of lysosomal cargo proteins.

To more comprehensively analyze how the loss of PIKfyve affects the contents secreted upon platelet activation, a quantitative proteomics analysis was performed. By tandem liquid chromatography- mass spectrometry (LC-MS/MS), we identified the proteins released from the control platelets and the PIKfyve-null platelets following thrombin stimulation. We then used the spectral counting of the identified peptides to quantitatively compare the proteins released from the control platelets and the PIKfyve-null platelets. Using a cutoff of 2.0-fold as a significant difference between them, we identified 17 proteins that were increased and 38 proteins that were decreased in the releasates of PIKfyve-null platelets relative to wild-type platelets (Supplementary table 1 and table 2). Among those proteins that were more abundant in the PIKfyve-null platelet releasates, several lysosomal enzymes stood out including cathepsin D, cathepsin B, and maltase (Supplementary table 1). Remarkably, levels of the cathepsin D were 20-fold higher in PIKfyve-null platelet releasates than in control releasates (Supplementary table 1). Further analysis of the sequence coverage and MS spectra of the tryptic peptides for cathepsin D demonstrated that the releasates of

PIKfyve-null platelets contained predominantly the procathepsin D - the immature and inactive proenzyme form of cathepsin D – but undetectable levels of mature cathepsin D (Supplementary Fig. 8a, 8b and 8c). To further validate these findings, we analyzed the expression of cathepsin D in platelet lysates by immunoblotting. Consistent with the proteomics data, both cathepsin D and procathepsin D were undedetectable in the lysates of wild-type platelets, and procathepsin D was highly elevated in PIKfyve-null platelets (Fig. 5d). These results suggest that cathepsin D expression is upregulated in PIKfyve-null platelets, but that the intracellular maturation of procathepsin D is defective in PIKfyve-null platelets. Consequently, cathepsin D activity was negligible in both the lysates and releasates of both wild-type and the PIKfyve-null platelets (data not shown). Together, these data demonstrate that PIKfyve ablation in platelets results in a defective lysosomal pathway reflected by abnormal storage, maturation, and release of lysosomal enzymes.

PIKfyve$^{fl/fl}$ Pf4-Cre mice develop accelerated arterial thrombosis upon vascular injury

Platelets have long been known to contain primary lysosomes and release their lysosomal enzymes in response to stimuli[30,31], but the physiologic role of platelet lysosome secretion has not been clearly delineated. Thus, we tested whether the lysosomal abnormalities observed in PIKfyve-null platelets correlated with any functional abnormalities. Washed platelets from control or PIKfyve$^{fl/fl}$ Pf4-cre mice formed aggregates to a similar degree in response to different agonists (data not shown), suggesting that activation of the dominant platelet integrin, αIIbβ3, is intact in the PIKfyve-null platelets. In addition, Akt phosphorylation was normally induced upon stimulation (Fig. 5f), suggesting that the intracellular signaling pathway in PIKfyve-null platelets is also preserved. To determine the effect of PIKfyve ablation in platelets during thrombosis *in vivo*, the carotid arteries of mice were analyzed for occlusive thrombus formation in response to a chemical injury with ferric chloride. At 12–16 weeks of age, PIKfyve$^{fl/fl}$ Pf4-Cre mice formed occluding thrombi significantly faster than their control littermates (3.8 ± 1.6 minutes vs. 6.1 ± 1.2 minutes, Fig. 5e). Since PIKfyve-null platelets showed normal aggregation *ex vivo*, we speculated that the excessive secretion of the platelet lysosomal contents from PIKfyve-null platelets could contribute to endothelial damage and systemic inflammation leading to accelerated thrombus formation. Consistent with this possibility, plasma levels of vWF, a marker of endothelial damage and systemic inflammation[32], were significantly elevated in the plasma of PIKfyve$^{fl/fl}$ Pf4-Cre mice when measured by immunoblotting (Fig. 5g) or ELISA (Fig. 5h). Together, these results suggest that excessive lysosomal secretion from PIKfyve-null platelets is associated with endothelial damage and systemic inflammation, perhaps underlying excessive thrombosis in PIKfyve$^{fl/fl}$ Pf4-Cre mice.

Impaired platelet lysosome secretion attenuates the phenotype of PIKfyve$^{fl/fl}$ Pf4-Cre mice

If the pathological macrophage inflammatory response in PIKfyve$^{fl/fl}$ Pf4-Cre mice reflects the excessive stimulus-induced secretion of lysosomal enzymes, we hypothesized that attenuating the release of platelet lysosomes would comparably attenuate the inflammatory responses. To test this hypothesis, PIKfyve$^{fl/fl}$ Pf4-Cre mice were crossed with *pallid* mice, a model of Hermansky-Pudlak Syndrome type 9[33]. *Pallid* mice lack an essential subunit of BLOC-1, a complex required for the biogenesis of lysosome-related organelles such as pigment cell melanosomes and platelet dense granules[34,35]. Importantly, stimulus-dependent

secretion of lysosomal contents is impaired (but not ablated) in platelets from *pallid* mice[36]. In contrast to PIKfyve$^{fl/fl}$ Pf4-Cre mice that developed persistent dorsal alopecia and weight gain, PIKfyve$^{fl/fl}$ Pf4-Cre/*pallid* mice maintained hair growth until death and exhibited attenuated weight gain (Fig. 6a and 6b; note that because the *pallid* mutation also impairs melanosome biogenesis, *pallid* mice exhibit hypopigmented fur). As expected, platelet and plasma levels of β-hexosaminidase were lower in PIKfyve$^{fl/fl}$ Pf4-Cre/*pallid* mice than in PIKfyve$^{fl/fl}$ Pf4-Cre mice (Fig. 6c and 6d). Together, these data suggest that the release of platelet lysosomes contributes to the pathogenesis of multiorgan defects in PIKfyve$^{fl/fl}$ Pf4-Cre mice.

Discussion

In this study, we show that PIKfyve kinase activity is critical in limiting the pathological inflammatory and thrombotic functions of platelet lysosomes. Our data indicate that PIKfyve kinase activity in platelets is essential for the normal maturation of cathepsin D and for the proper storage and release of lysosomal enzymes. Unexpectedly, dysregulated lysosomal homeostasis and enhanced lysosomal release from PIKfyve-null platelets drive an aberrant inflammatory response in macrophages. This leads to chronic inflammation and arterial thrombosis that affect the development, body mass, fertility, and survival of mice.

Our study shows that PIKfyve-null platelets excessively accumulate lysosomal components, which include lysosomal membrane proteins as well as lysosomal enzymes such as β-hexosaminidase and procathepsin D. Procathepsin D is targeted from the TGN to endosomes primarily via the mannose-6-phosphate receptor (M6PR) pathway, and is further processed to active cathepsin D in acidic lysosomes[37]. The M6PR must then recycle to the TGN for another round of transport. The excessive accumulation and release of procathepsin D in PIKfyve-null platelets suggests that PIKfyve is critical for procathepsin D trafficking from the TGN to endosomes. This conclusion is consistent with a published study showing that PtdIns(3,5)P_2 deficiency leads to the defective retrograde trafficking of M6PR from endosomes to the TGN[38], which would ultimately exhaust the M6PR from the TGN and result in default secretion of procathepsin D. Similarly, cultured fibroblasts derived from Vac14-null mice develop defective steady-state localization of M6PR, and these fibroblasts also accumulate the immature forms of cathepsin D[13]. However, PtdIns(3,5)P_2 is also required for acidification of the lysosome-like vacuole in yeast[9]. Because the low pH in lysosomes is essential for the proteolytic maturation of procathepsin D, an abnormal lysosomal pH could contribute to the defective processing of procathepsin D in the PIKfyve-null platelets. In addition, wild-type platelets contain and secrete only minor amounts of procathepsin D[39] whereas PIKfyve-null platelets excessively store and release procathepsin D. This suggests that PtdIns(3,5)P_2 deficiency might additionally feed back on lysosomal enzyme biosynthesis, perhaps by activating the CLEAR (coordinated lysosomal expression and regulation) gene network[40,41].

Interestingly, overexpression and secretion of procathepsin D have been found in several human cancers, including in breast and in lung carcinoma[42]. In these tumor cells, alterations of pathways that are M6PR dependent and independent have both been suggested[43,44]. In addition, excessive release of the lysosomal enzymes are also seen in the lysosomal storage

disorders, Mucolipidosis II and Mucolipidosis III[45]. In these diseases, an inability to generate the M6P recognition signal on the lysosomal enzymes impairs their delivery from the TGN to the lysosome via the M6PR pathway resulting in the excessive release of lysosomal enzymes extracellularly[46]. Thus, the absence of PIKfyve in platelets results in a phenotype that is reminiscent of several human disorders with impaired trafficking from the TGN to the lysosome.

Similar to PIKfyve deficiency, the deficiency of the inositol phosphatase and PIKfyve chaperone protein called Fig4 results in the reduced intracellular PtdIns(3,5)P_2 concentrations. Notably, Fig 4-deficient mice develop enlarged endolysosomal vacuoles and excessive accumulation of lysosomal proteins, reminiscent of lysosomal storage diseases [47]. Likewise, mice lacking another PIKfyve-binding partner called Vac14 have decreased synthesis of PtdIns(3,5)P_2 and develop excessive vacuolation of late endosomal and lysosomal compartments[13]. Together with our findings, these studies further support that the depletion of PtdIns(3,5)P_2 by impairing any components of the PIKfyve complex could lead to the features that are reminiscent of those found in lysosomal storage disorders.

It is notable that lysosomal storage diseases are frequently associated with inappropriate immune responses that result in chronic inflammation. For example, tissue infiltration of reactive macrophages can lead to visceral organomegaly in both Gaucher and Niemann-Pick diseases[48,49]. Likewise, microglial activation is frequently associated with the neuropathology in mucopolysaccaridoses[50]. Ablation of PIKfyve in platelets causes similar inflammatory responses that are associated with robust macrophage defects, which lead to organomegaly in mice. Using several lines of evidence, we demonstrated that this macrophage phenotype is non-cell-autonomous, showing that PIKfyve-null platelets can induce aberrant responses in normal macrophages. A similar non-cell-autonomous phenomenon has also been observed in Fig4-null mice. Fig4-null mice have a neurodegenerative disorder[14]. The genetic restoration of Fig4 exclusively in the neuronal cells of Fig4-null mice not only reverts the dysfunctions of neuronal cells, but it also reverts the dysfunctions of the adjacent oligodendrocytes including hypomyelination and maturation defects[51]. Interestingly, the inflammatory response seen in PIKfyve$^{fl/fl}$ Pf4-Cre mice has not been described in mice lacking either Fig4 or Vac14. This could be due to the fact that Fig4- or Vac14-null mice do not survive long enough to fully develop the robust tissue accumulation of macrophages seen in PIKfyve$^{fl/fl}$ Pf4-Cre mice. These studies taken together indicate that the depletion of PtdIns(3,5)P_2 in a single cell type may have indirect implications in other cell types. Furthermore, they also show that our findings are consistent with the broad secondary defects shown in lysosomal storage disorders.

Megakaryocytes and platelets have long been known to possess lysosomes that contain different hydrolases including proteases and glycosidases.[30,52] Upon platelet activation *in vivo*, platelets release not only alpha granules and dense granules, but they also release their lysosomal contents.[53] The physiopathological role of platelet lysosome secretion is not well understood. However, it has been speculated that the release of platelet lysosomal enzymes may be required for the remodeling of extracellular matrix during wound healing[54]. In addition, the pathological release of lysosomal enzymes may also cause the local injury of the vascular wall leading to atherosclerosis and the focal thickening of arteries[55]. Thus,

proper regulation of the platelet lysosomal secretion would be essential to maintain a normal response to wound healing, and also to avoid the inflammatory and thrombotic defects that could result from the excessive platelet lysosomal secretion. Consistent with this concept, this study shows that the excessive storage and secretion of lysosomal enzymes from platelets lacking PIKfyve result in the accelerated arterial thrombosis and inflammation observed in PIKfyve$^{fl/fl}$ Pf4-Cre mice. Thus, our studies further support that the proper regulation of platelet lysosomal storage and secretion play a crucial role in limiting the proinflammatory and prothrombotic functions of platelets.

Our study demonstrates the novel finding that PIKfyve kinase activity is a critical regulator of the lysosomal pathway in mouse platelets. This work also provides evidence that in addition to the effects mediated by the release of platelets alpha and dense granules, secretion of platelet lysosomes may be a previously unrecognized initiator of vascular damage and inflammatory responses. These findings could have important implications and applications in the diagnosis and in the design of novel targets for clinical disorders mediated by platelets.

Methods

Animal models

Targeting of the PIKfyve gene was generated using C57BL6 mice (inGenious Targeting Laboratory). A bacterial artificial chromosome (BAC) derived from C47BL/6 (RPCI23) genomic DNA was used to construct the targeting vector. The targeting vector was designed to excise exons 37 and 38 of the mouse PIKfyve gene that encodes the activation loop of the kinase domain. The 7.55 kb long homology arm extended 5’ to exon 37, and the 1.5kb short homology arm extended 3’ to exon 38. The loxP flanked Neo cassette was inserted on the 3’ side of exon 38, and the single loxP site was inserted at the 5’ side of exon 37. The resulting 10.6kb fragment was subcloned into an approximately 2.4kb backbone vector (pSP72, Promega) containing an ampicillin selection cassette to generate a final targeting construct of 14.8kb. C57BL/6 embryonic stem cells were electroporated with targeting vectors. Clones resistant to the G418 antibiotic were selected and screened by Southern Blot and PCR. For Southern Blot, a probe that targeted downstream of the exon 39 was used. PCR primers were designed to amplify a segment of the neomycin cassette (A1 and LAN1). The selected clones were microinjected into C57BL/6 blastocysts. Resulting chimeras with black coat color were mated with wild-type C57BL/6 mice to generate PIKfyve F1 heterozygous offspring. Tail DNA was used to genotype these mice by PCR using the same primers designed to select the recombinant ES clones (A1 and LAN1). F1 heterozygous mice were crossed with a FLP transgenic mouse to excise the neomycin cassette that was flanked by FRT sites. The resulting F2 mosaic offspring were crossed with wild-type mice to generate F3 heterozygotes that were missing the neomycin cassette. F3 heterozygotes were crossed to generate mice carrying the PIKfyve floxed allele (PIKfyve^{fl}). PIKfyve$^{fl/fl}$ mice were crossed with transgenic mice expressing Cre recombinase under the control of the platelet factor 4 promoter (Pf4-Cre) to induce tissue-restricted Cre recombination in the megakaryocyte lineage. For some experiments, PIKfyve$^{fl/fl}$ mice were crossed with a B6;129S4-*Gt(ROSA)26Sor*^{tm1Sor}/J (Rosa26-LacZ) reporter strain and then with a Pf4-Cre transgenic

mouse. For other experiments, PIKfyve$^{fl/fl}$ mice were crossed with B6-Cg-*Pldn*^{pa}/J (*pallid*) mice, and their offspring were paired with the Pf4-Cre transgenic mice to generate PIKfyve$^{fl/fl}$ Pf4-Cre/*pallid* mice. Animals were maintained on standard chow and tap water according to the Institutional Animal Care and Use Committees of the University of Pennsylvania. Genomic DNA isolated from tail biopsies was used for the genotyping of alleles of the PIKfyve gene by PCR using forward primer (5'-CCATTGCCTGGCTTAGAACAGAG-3') and reverse primer (5'-GAACTCTCCCGCGTAGTACAGC-3'). PCR generated products were either 310 bp corresponding to the wild-type alleles or 370 bp corresponding to the targeted allele.

Body composition analysis

Mice were anesthesized with sodium pentobarbital (90mg/kg) and scanned by dual energy X-ray absorptiometry (DEXA) at the Mouse Metabolism Core at the University of Pennsylvania.

Histopathology, immunohistochemistry, and X-gal staining

Necropsies were performed on approximately 50 control mice and 50 PIKfyve$^{fl/fl}$ Pf4-Cre mice between 3 weeks and 28 weeks of age. They included macroscopic observations, body and organ weight measurements, complete blood counts, serum chemistry analysis, and microscopic examination of the brain, thymus, lymph nodes, heart, lung, small intestine, large intestine, liver, spleen, pancreas, kidney, ovaries, testis, skin, muscle, fat, and bone marrow. Fresh postmortem tissues were fixed overnight in 10% formalin, paraffin-embedded, sectioned, and stained with hematoxylin/eosin, PAS, Alcian Blue, and Trichrome Mason. Frozen tissue sections were fixed with formalin for 5 minutes and stained for oil red O. For immunohistochemistry, frozen tissue sections were fixed with 4% paraformaldehyde for 5 minutes, and stained with F4/80 (Serotec; 1:100), CD41 (BD Pharmingen; MWReg30; 1:50), and CD45R/B220 (BD Pharmingen; RA3–6B2; 1:500). For X-gal staining, frozen tissue sections were fixed with 0.5% glutaraldehyde for 10 minutes, and stained overnight with the chromogenic substrate for β-galactosidase, X-gal (Cell Center, University of Pennsylvania).

Immunoblotting

Tissues were harvested and homogenized in RIPA buffer with a protease inhibitor cocktail (Roche). The protein concentrations were determined using the BCA Protein Assay (Pierce). Proteins were separated on SDS-PAGE gradient gels (Invitrogen) and then transferred onto the polyvinylidene difluoride membrane (Invitrogen). The membrane was blotted with the indicated primary antibodies against: PIKfyve-N-terminal (Sigma-Aldrich; P0054; 1:400), LAMP-1 (Developmental Studies Hybridoma Bank; 1:1000), EEA-1 (Santa Cruz; 1:1000), Cathepsin D (Calbiochem; 1:1000), vWF (DAKO; 1:1000), PF4 (Bethyl; 1:1000), Akt (Cell Signaling Technology; 1:1000), pAkt (Cell Signaling Technology; 1:1000), and Actin (Cell Signaling Technology; 1:1000). This was followed by blotting with horseradish peroxidase conjugated secondary antibodies and developing with enhanced chemiluminescence substrate (GE Healthcare).

Megakaryocyte and platelet preparation

Megakaryocytes were derived from the bone marrow of mice in the presence of thrombopoietin (TPO), as previously described[26]. Briefly, bone marrow cells were collected by flushing mouse femurs and cultured in the presence of 1% TPO. After 4 days, cultured megakaryocytes were isolated by sedimentation through a 1.5%/3% BSA step gradient. Washed platelets were prepared as previously described[25]. Blood was collected from the inferior vena cava of mice into 0.1 volume of acid citrate dextrose buffer. Platelet-rich plasma was separated by centrifugation at 200g for 10 minutes and incubated with 1uM prostaglandin E1 for 10 minutes at room temperature. Platelets were then isolated by centrifugation at 800g for 10 minutes and resuspended in HEPES-Tyrode buffer pH 7.4.

Megakaryocyte number and ploidy analysis

To measure the number of megakaryocytes in the bone marrow, isolated megakaryocytes from the bone marrow were stained with CD41 antibody conjugate with Alexa 488 (BD Biosciences), and cells were counted on the FACS Calibur flow cytometer (BD Biosciences) discriminating size to subtract out platelets. To determine the megakaryocyte ploidy, cells were stained with propidium iodide and the relative DNA content was measured. FlowJo software was used to analyze all flow cytometry data.

P-selectin expression analysis

Platelets were diluted to a density of 5×10^6 cells/ml, stimulated with thrombin at indicated concentrations and then incubated with a phycoerythrin-conjugated P-selectin antibody (BD Pharmigen). Fluorescence values were analyzed on a FACS Calibur flow cytometer (BD Biosciences).

Transmission electron microscopy

Megakaryocytes grown in culture were harvested on day 6 and fixed in glutaraldehyde. Ultrathin sections were obtained and collected on hexagonal copper grids. Sections were stained with Reynold's lead citrate and examined using transmission electron microscopy at the Electron Microscopy Core Facility at the University of Pennsylvania.

Platelet depletion *in vivo*

To study the effects of platelet depletion in the control mice and the PIKfyve $^{fl/fl}$ Pf4-Cre mice, mice at 10–12 weeks of age were administered with 2μg/g of GPIbα antibody (Emfret) twice weekly by intraperitoneal injections for a total of 6 weeks. Blood counts were monitored weekly by collecting blood from the retro-orbital sinuses. Body weight was monitored twice weekly. Necropsies were performed at the completion of 6 weeks of antibody treatment.

Radiation bone marrow chimeras

Bone marrow cells were isolated from wild-type mice expressing either CD45.1 or CD45.2 congenic markers or from PIKfyve$^{fl/fl}$ Pf4-Cre mice expressing CD45.2 congenic markers. Bone marrow cells were depleted from T cells and red blood cells by using magnetic beads bound to antibodies against Ter119, CD3, CD4, and CD8. To study the phenotype rescue

effect, PIKfyve$^{fl/fl}$ Pf4-Cre recipient mice expressing CD 45.2 congenic markers were irradiated with 900 rads and administered by retro orbital injection with 2×10^6 bone marrow cells from wild-type mice expressing CD 45.1 markers. To study the phenotype transfer effect, wild-type recipient mice expressing CD45.1 markers were irradiated with 900 rads, and administered by retro orbital injection with 1×10^6 bone marrow cells from wild-type mice expressing thy 1.1 marker and 1×10^6 bone marrow cells from PIKfyve$^{fl/fl}$ Pf4-Cre mice expressing CD 45.2 markers. Transplanted mice were maintained in sterile water with sulfamethoxazole/trimethoprim for 3 weeks. Mice were sacrificed, and analyzed for engraftment and histology analyses at about 33–35 weeks after transplantation.

Acid hydrolases assays

The activity of β-hexosaminidase was determined as described previously[27]. Platelets or plasma were extracted from mice and mixed with 10mM substrate (p-nitrophenyl-N-acetyl-β-D-glucosaminide) in citrate-phosphate buffer pH 4.5. Platelet extracts were incubated for 16 hours at 37°C, and plasma was incubated for 1 hour at 37°C. The enzymatic reaction was stopped by the addition of 0.5M NaOH. The absorbance of released p-nitrophenolate was read at 405nm in an ELISA plate reader.

$FeCl_3$-induced carotid artery thrombosis assay

Mice were anesthetized using sodium pentobarbital (90 mg/kg). A midline incision was made in the neck, and the carotid artery was exposed and dissected away from surrounding tissue. The artery was placed on a Doppler flow probe (Transonic Systems, Ithaca, NY) to monitor blood flow through the vessel. After a baseline flow measurement was recorded, vascular injury was initiated by placing a 1 mm^2 piece of filter paper saturated with 7.5% $FeCl_3$ (Sigma) on the surface of the artery for 2 minutes. The filter paper was then removed and the artery rinsed with saline, followed by the continuous recording of blood flow in the vessel for 20 minutes post-injury. The time to vessel occlusion was recorded.

Plasma vWF analysis

For analysis of plasma vWF multimer distribution, mouse plasma (10μl) was denatured at 60°C for 20 minutes with 10μl of sample buffer (70mM Tris, pH 6.8, 2.4% SDS, 0.67M urea, 4mM EDTA, 10% glycerol, 0.01% bromophenol blue). Proteins were fractionated on 1% agarose gel on ice and transferred to a nitrocellulose membrane. The membrane was blotted with vWF IgG antibody (Dako; 1:5000) to detect the vWF multimers. For quantification analysis of plasma vWF antigen, we performed ELISA as described previously. Briefly, a microtiter plate coated with rabbit anti-vWF IgG (Dako; 1:2000) was incubated with diluted mouse plasma for 1 hour at room temperature. After washing with PBS, bound vWF was determined by peroxidase-conjugated rabbit anti-vWF IgG (Dako; 1:2000). A pre-mixed TMB solution was used for color development. The absorbance at 450nm was determined by an ELISA plate reader.

Mass spectrometry analysis

To prepare platelet releasates for proteomics analysis, washed platelets (5×10^8 cells/ml) were stimulated with 1U/mL thrombin for 10 minutes at 37°C. Activated platelets were

centrifuged at 13,000g for 10 minutes at 4°C and the supernates were isolated from the pellets. The concentrations of proteins from the platelet supernates were measured using the BCA protein assay (Pierce). Proteins (40ug) were digested with trypsin in solution. Tryptic digests were analyzed by LC-MS/MS on a hybrid LTQ Orbitrap Elite mass spectrometer (Thermofisher Scientific San Jose, CA) coupled with a nano LC Ultra (Eksigent). Peptides were separated by reverse phase (RP)-HPLC on a nanocapillary column, 75 μm id × 15 cm Reprosil-pur 3uM (Dr. Maisch, Germany) in a Nanoflex chip system (Eksigent). Mobile phase A consisted of 1% methanol (Fisher)/0.1% formic acid (Thermo) and mobile phase B of 1% methanol/0.1% formic acid/80% acetonitrile. Peptides were eluted into the mass spectrometer at 300 nL/min with each RP-LC run comprising a 90 minute gradient from 10 to 25 % B in 65 min, 25–40%B in 25 min. The mass spectrometer was set to repetitively scan m/z from 300 to 1800 (R = 240,000 for LTQ-Orbitrap Elite) followed by data-dependent MS/MS scans on the twenty most abundant ions, with a minimum signal of 5000, dynamic exclusion with a repeat count of 1, repeat duration of 30s, exclusion size of 500 and duration of 60s, isolation width of 2.0, normalized collision energy of 33, and waveform injection and dynamic exclusion enabled. FTMS full scan AGC target value was 1e6, while MSn AGC was 1e4, respectively. FTMS full scan maximum fill time was 500 ms, while ion trap MSn fill time was 50 ms; microscans were set at one. FT preview mode; charge state screening, and monoisotopic precursor selection were all enabled with rejection of unassigned and 1+ charge states.

For database search, MS/MS raw files were searched against a mouse protein sequence database including isoforms from the Uniprot Knowledgebase (taxonomy:10090 AND keyword: "Complete proteome [KW-0181]") using MaxQuant version 1.4.1.2 with the following set parameters: Fixed modifications, Carbamidomethyl (C); Decoy mode, revert; MS/MS tolerance ITMS, 0.5 Da; false discovery rate for both peptides and proteins, 0.01; Minimum peptide Length, 6; Modifications included in protein quantification, Acetyl (Protein N-term), Oxidation (M); Peptides used for protein quantification, Razor and unique. The numbers of peptide spectral matches to each protein were used for quantitative comparison between samples as described below.

For statistical analysis of mass spectrometry data, we adapted a method proposed by Choi[56] to use the number of peptide spectral matches (PSMs) in each protein to determine the likelihood that the protein was differentially regulated across the control mice and the knockout mice. The idea is to develop a control model and a knockout model, and for each protein test whether the knockout model describes its expression data significantly better than the control model. To do so, we estimate a Bayes Factor $B_p = \frac{P(M^k|Data)}{P(M^c|Data)}$ for each protein. We assume that the number of PSMs for protein *p* in sample *i* can be modeled as a Poisson distribution with mean $\lambda_{p,i,}$ since each element $x_{p,i,}$ in the PSM data matrix *X* is count data. To combat the limited number of biological replicates in each treatment group, we pooled information across replicates and estimate each $\lambda_{p,i,}$ using a control and knockout hierarchical log-linear model, denoted by:

$$M^c: log(\lambda^c_{p,i}) = log(L_p) + log(N_i) + a_0 + c_p \quad M^k: log(\lambda^k_{p,i}) = log(L_p) + log(N_i) + a_0 + c_p + T_i k_p,$$

, where L_p is the length of protein p, N_i is the mean number of spectral counts in sample i, $T_i = \begin{cases} 0 \text{ if sample } i \text{ is a control mouse} \\ 1 \text{ if sample } i \text{ is a knockout mouse} \end{cases}$, a_0 is a model constant, c_p is a protein's native expression term, and k_p is a protein's knockout expression term. We give the model a well-defined structure by putting priors on $a_0 \sim N(0,\delta_a^2)$, $c_p \sim N(0,\delta_c^2)$ and $k_p \sim N(0,\delta_k^2)$. To make data-driven estimates of δ_c^2 and δ_k^2, we place hyper priors on these two parameters, given by ${}^{1}\!/_{\delta_c^2}, {}^{1}\!/_{\delta_k^2} \sim Gamma(0.1, 0.1)$. We let a_0 "float", and thus set $\delta_a^2 = 10^2$. We use these parameters (denoted as a vector by $\vec{\theta}$) to estimate the Bayes Factor

$$B_p = \frac{P(M^k|X)}{P(M^c|X)} = \frac{\int P(X|M^k,\vec{\theta}^k)P(\vec{\theta}^k|M^k)d\vec{\theta}^k}{\int P(X|M^c,\vec{\theta}^c)P(\vec{\theta}^c|M^c)d\vec{\theta}^c}\frac{P(M^k)}{P(M^c)} = \frac{E_{\vec{\theta}^k|M^k}[P(X|M^k,\vec{\theta}^k)]}{E_{\vec{\theta}^c|M^c}[P(X|M^c,\vec{\theta}^c)]}$$

(assuming we have no prior knowledge of $P(M^k) \text{and} P(M^c) \text{for any protein} = \frac{\lim_{N\to\infty}\frac{1}{N}\sum_{n=1}^{N}P(X|M^k,\vec{\theta}^k_n)}{\lim_{N\to\infty}\frac{1}{N}\sum_{n=1}^{N}P(X|M^c,\vec{\theta}^c_n)}$, where the transition states $\vec{\theta}_n \to \vec{\theta}_{n+1}$ are determined using Metropolis Hastings and Gibbs Sampling Markov Chain Monte Carlo techniques. Specifically, at iteration n with parameter vector $\vec{\theta}^k_n$ (we explain using the knockout model, since $M^c \subset M^k$),

$$P\left(a_{0_n}|\cdot\right) \alpha P\left(X\middle|a_{0_n},\cdot\right) P\left(a_{0_n}\right) = Poisson\left(X\middle|a_{0_n},\cdot\right) N\left(a_{0_n};0,{\delta_a}^2\right)$$

$$P\left(c_{p_n}\middle|\cdot\right) \alpha P\left(X\middle|c_{p_n},\cdot\right) P\left(c_{p_n}\right) = Poisson\left(X\middle|c_{p_n},\cdot\right) N\left(c_{p_n};0,{\delta_c}^2\right)$$

$$P\left(k_{p_n}\middle|\cdot\right) \alpha P\left(X\middle|k_{p_n},\cdot\right) P\left(k_{p_n}\right) = Poisson\left(X\middle|k_{p_n},\cdot\right) N\left(k_{p_n};0,{\delta_k}^2\right)$$

$$P\left({\delta_c}^2{}_n\middle|\cdot\right) \alpha P\left(\{c_p\}_{p=1}^{G}\middle|{\delta_c}^2{}_n\right) P\left({\delta_c}^2{}_n\right) = InvGamma\left(0.1+\frac{G}{2}, 0.1+\frac{\sum_{p=1}^{G}{c_p}^2}{2}\right), G = \#\text{proteins}$$

$$P\left({\delta_k}^2{}_n\middle|\cdot\right) \alpha P\left(\{k_p\}_{p=1}^{G}\middle|{\delta_k}^2{}_n P\left({\delta_k}^2{}_n\right)\right) = InvGamma\left(0.1+\frac{G}{2}, 0.1+\frac{\sum_{p=1}^{G}{k_p}^2}{2}\right).$$

To determine the set of proteins that significantly changed in the knockout set with respect to the control set, we imposed a strict cutoff and required that each protein have a Bayes Factor of at least 8 and a fold change of at least 2.0.

Statistical analysis

GraphPad Prism 5 was used to analyze data. All data are presented as mean +/− S.D. Two-tailed Student's t-tests were used for the comparison of two groups. Two-sided analysis of variance with Bonferroni correction was used for the comparison of more than 2 groups. A log rank test was performed for Kaplan Meier survival analysis. *P*-values of <0.05 (*), <0.01 (**), and < 0.001(***) were used to ascertain statistical significance.

Supplementary Material

Refer to Web version on PubMed Central for supplementary material.

Acknowledgements

This work was supported by the NHLBI T32 Training Grant, PO1 HL40387, R01HL110110, the NIH/NIDDK Center for Molecular Studies in Digestive and Liver Diseases (P30-DK050306) and its Core Facilities (Molecular Pathology and Imaging). We thank Skip Brass, Mark Kahn, Edward Behrens, Claudio Giraudo and Long Zheng for their thoughtful discussions. We also thank Lynn A. Spruce for expert technical assistance with mass spectrometry.

References

1. Di Paolo G, De Camilli P. Phosphoinositides in cell regulation and membrane dynamics. Nature. 2006; 443:651–657. [PubMed: 17035995]
2. McCrea HJ, De Camilli P. Mutations in phosphoinositide metabolizing enzymes and human disease. Physiology. 2009; 24:8–16. [PubMed: 19196647]
3. Shisheva A. PIKfyve: Partners, significance, debates and paradoxes. Cell biology international. 2008; 32:591–604. [PubMed: 18304842]
4. Gary JD, et al. Regulation of Fab1 phosphatidylinositol 3-phosphate 5-kinase pathway by Vac7 protein and Fig4, a polyphosphoinositide phosphatase family member. Molecular biology of the cell. 2002; 13:1238–1251. [PubMed: 11950935]
5. Sbrissa D, et al. Core protein machinery for mammalian phosphatidylinositol 3,5-bisphosphate synthesis turnover that regulates the progression of endosomal transport Novel Sac phosphatase joins the ArPIKfyve-PIKfyve complex. The Journal of biological chemistry. 2007; 282:23878–23891. [PubMed: 17556371]
6. Jin N, et al. VAC14 nucleates a protein complex essential for the acute interconversion of PI3P and PI(3,5)P(2) in yeast and mouse. The EMBO journal. 2008; 27:3221–3234. [PubMed: 19037259]
7. Sbrissa D, Ikonomov OC, Fenner H, Shisheva A. ArPIKfyve homomeric and heteromeric interactions scaffold PIKfyve and Sac3 in a complex to promote PIKfyve activity and functionality. Journal of molecular biology. 2008; 384:766–779. [PubMed: 18950639]
8. Dove SK, Dong K, Kobayashi T, Williams FK, Michell RH. Phosphatidylinositol 3,5-bisphosphate and Fab1p/PIKfyve underPPIn endo-lysosome function. The Biochemical journal. 2009; 419:1–13. [PubMed: 19272020]
9. McCartney AJ, Zhang Y, Weisman LS. Phosphatidylinositol 3,5-bisphosphate: Low abundance, high significance. BioEssays: news and reviews in molecular, cellular and developmental biology. 2014; 36:52–64.
10. Takasuga S, Sasaki T. Phosphatidylinositol-3,5-bisphosphate: metabolism and physiological functions. Journal of biochemistry. 2013; 154:211–218. [PubMed: 23857703]
11. Ikonomov OC, et al. The phosphoinositide kinase PIKfyve is vital in early embryonic development: preimplantation lethality of PIKfyve−/− embryos but normality of PIKfyve+/− mice. The Journal of biological chemistry. 2011; 286:13404–13413. [PubMed: 21349843]
12. Zolov SN, et al. In vivo, Pikfyve generates PI(3,5)P2, which serves as both a signaling lipid and the major precursor for PI5P. Proceedings of the National Academy of Sciences of the United States of America. 2012; 109:17472–17477. [PubMed: 23047693]
13. Zhang Y, et al. Loss ofVac14, a regulator of the signaling lipid phosphatidylinositol 3,5-bisphosphate, results in neurodegeneration in mice. Proceedings of the National Academy of Sciences of the United States of America. 2007; 104:17518–17523. [PubMed: 17956977]
14. Chow CY, et al. Mutation of FIG4 causes neurodegeneration in the pale tremor mouse and patients with CMT4J. Nature. 2007; 448:68–72. [PubMed: 17572665]
15. Chow CY, et al. Deleterious variants of FIG4, a phosphoinositide phosphatase, in patients with ALS. American journal of human genetics. 2009; 84:85–88. [PubMed: 19118816]
16. Min SH, Abrams CS. Regulation of platelet plug formation by phosphoinositide metabolism. Blood. 2013; 122:1358–1365. [PubMed: 23757731]

17. King SM, Reed GL. Development of platelet secretory granules. Seminars in cell & developmental biology. 2002; 13:293–302. [PubMed: 12243729]
18. Whiteheart SW. Platelet granules: surprise packages. Blood. 2011; 118:1190–1191. [PubMed: 21816838]
19. Heijnen HF, et al. Multivesicular bodies are an intermediate stage in the formation of platelet alpha-granules. Blood. 1998; 91:2313–2325. [PubMed: 9516129]
20. Youssefian T, Cramer EM. Megakaryocyte dense granule components are sorted in multivesicular bodies. Blood. 2000; 95:4004–4007. [PubMed: 10845941]
21. Ambrosio AL, Boyle JA, Di Pietro SM. Mechanism of platelet dense granule biogenesis: study of cargo transport and function of Rab32 and Rab38 in a model system. Blood. 2012; 120:4072–4081. [PubMed: 22927249]
22. Meng R, et al. SLC35D3 delivery from megakaryocyte early endosomes is required for platelet dense granule biogenesis and is differentially defective in Hermansky-Pudlak syndrome models. Blood. 2012; 120:404–414. [PubMed: 22611153]
23. Tiedt R, Schomber T, Hao-Shen H, Skoda RC. Pf4-Cre transgenic mice allow the generation of lineage-restricted gene knockouts for studying megakaryocyte and platelet function in vivo. Blood. 2007; 109:1503–1506. [PubMed: 17032923]
24. Bertozzi CC, et al. Platelets regulate lymphatic vascular development through CLEC-2-SLP-76 signaling. Blood. 2010; 116:661–670. [PubMed: 20363774]
25. Carramolino L, et al. Platelets play an essential role in separating the blood and lymphatic vasculatures during embryonic angiogenesis. Circulation research. 2010; 106:1197–1201. [PubMed: 20203303]
26. Josefsson EC, et al. Megakaryocytes possess a functional intrinsic apoptosis pathway that must be restrained to survive and produce platelets. J Exp Med. 2011; 208:2017–2031. [PubMed: 21911424]
27. Soriano P. Generalized lacZ expression with the ROSA26 Cre reporter strain. Nature genetics. 1999; 21:70–71. [PubMed: 9916792]
28. Nieswandt B, Bergmeier W, Rackebrandt K, Gessner JE, Zirngibl H. Identification of critical antigen-specific mechanisms in the development of immune thrombocytopenic purpura in mice. Blood. 2000; 96:2520–2527. [PubMed: 11001906]
29. Bergmeier W, Rackebrandt K, Schroder W, Zirngibl H, Nieswandt B. Structural and functional characterization of the mouse von Willebrand factor receptor GPIb-IX with novel monoclonal antibodies. Blood. 2000; 95:886–893. [PubMed: 10648400]
30. Bentfeld-Barker ME, Bainton DF. Identification of primary lysosomes in human megakaryocytes and platelets. Blood. 1982; 59:472–481. [PubMed: 6277410]
31. Rendu F, et al. Signal transduction in normal and pathological thrombin-stimulated human platelets. Biochimie. 1987; 69:305–313. [PubMed: 3115311]
32. Lip GY, Blann A. von Willebrand factor: a marker of endothelial dysfunction in vascular disorders? Cardiovascular research. 1997; 34:255–265. [PubMed: 9205537]
33. Cullinane AR, et al. A BLOC-1 mutation screen reveals that PLDN is mutated in Hermansky-Pudlak Syndrome type 9. American journal ofhuman genetics. 2011; 88:778–787.
34. Wei AH, Li W. Hermansky-Pudlak syndrome: pigmentary and non-pigmentary defects and their pathogenesis. Pigment cell & melanoma research. 2013; 26:176–192. [PubMed: 23171219]
35. Marks MS, Heijnen HF, Raposo G. Lysosome-related organelles: unusual compartments become mainstream. Current opinion in cell biology. 2013
36. Novak EK, Hui SW, Swank RT. Platelet storage pool deficiency in mouse pigment mutations associated with seven distinct genetic loci. Blood. 1984; 63:536–544. [PubMed: 6696991]
37. Kornfeld S. Trafficking of lysosomal enzymes. FASEB journal: official publication of the Federation of American Societies for Experimental Biology. 1987; 1:462–468. [PubMed: 3315809]
38. Rutherford AC, et al. The mammalian phosphatidylinositol 3-phosphate 5-kinase (PIKfyve) regulates endosome-to-TGN retrograde transport. Journal of cell science. 2006; 119:3944–3957. [PubMed: 16954148]

39. Benes P, Vetvicka V, Fusek M. Cathepsin D--many functions of one aspartic protease. Critical reviews in oncology/hematology. 2008; 68:12–28. [PubMed: 18396408]
40. Sardiello M, et al. A gene network regulating lysosomal biogenesis and function. Science. 2009; 325:473–477. [PubMed: 19556463]
41. Settembre C, Fraldi A, Medina DL, Ballabio A. Signals from the lysosome: a control centre for cellular clearance and energy metabolism. Nature reviews. Molecular cell biology. 2013; 14:283–296.
42. Vetvicka V, Vashishta A, Saraswat-Ohri S, Vetvickova J. Procathepsin D and cancer: From molecular biology to clinical applications. World journal of clinical oncology. 2010; 1:35–40. [PubMed: 21603309]
43. Mathieu M, Vignon F, Capony F, Rochefort H. Estradiol down-regulates the mannose-6-phosphate/insulin-like growth factor-II receptor gene and induces cathepsin-D in breast cancer cells: a receptor saturation mechanism to increase the secretion of lysosomal proenzymes. Molecular endocrinology. 1991; 5:815–822. [PubMed: 1656243]
44. Isidoro C, Baccino FM, Hasilik A. Mis-sorting of procathepsin D in metastogenic tumor cells is not due to impaired synthesis of the phosphomannosyl signal International journal of cancer. Journal international du cancer. 1997; 70:561–566. [PubMed: 9052756]
45. Platt FM, Boland B, van der Spoel AC. The cell biology of disease: lysosomal storage disorders: the cellular impact of lysosomal dysfunction. The Journal of cell biology. 2012; 199:723–734. [PubMed: 23185029]
46. Vogel P, et al. Comparative pathology of murine mucolipidosis types II and IIIC. Veterinary pathology. 2009; 46:313–324. [PubMed: 19261645]
47. Zhang X, et al. Mutation of FIG4 causes a rapidly progressive, asymmetric neuronal degeneration. Brain : a journal of neurology. 2008; 131:1990–2001. [PubMed: 18556664]
48. Vitner EB, Platt FM, Futerman AH. Common and uncommon pathogenic cascades in lysosomal storage diseases. The Journal of biological chemistry. 2010; 285:20423–20427. [PubMed: 20430897]
49. Boven LA, et al. Gaucher cells demonstrate a distinct macrophage phenotype and resemble alternatively activated macrophages. American journal of clinical pathology. 2004; 122:359–369. [PubMed: 15362365]
50. Parkinson-Lawrence EJ, et al. Lysosomal storage disease: revealing lysosomal function and physiology. Physiology. 2010; 25:102–115. [PubMed: 20430954]
51. Winters JJ, et al. Congenital CNS hypomyelination in the Fig4 null mouse is rescued by neuronal expression of the PI(3,5)P(2) phosphatase Fig4. The Journal of neuroscience: the official journal of the Society for Neuroscience. 2011; 31:17736–17751. [PubMed: 22131434]
52. Bentfeld ME, Bainton DF. Cytochemical localization of lysosomal enzymes in rat megakaryocytes and platelets. The Journal of clinical investigation. 1975; 56:1635–1649. [PubMed: 1202088]
53. Ciferri S, et al. Platelets release their lysosomal content in vivo in humans upon activation. Thrombosis and haemostasis. 2000; 83:157–164. [PubMed: 10669170]
54. Rendu F, Brohard-Bohn B. The platelet release reaction: granules' constituents, secretion and functions. Platelets. 2001; 12:261–273. [PubMed: 11487378]
55. Muir EM, Bowyer DE. Inhibition of pinocytosis and induction of release of lysosomal contents by lysosomal overload of arterial smooth muscle cells in vitro. Atherosclerosis. 1984; 50:85–92. [PubMed: 6696784]
56. Choi H, Fermin D, Nesvizhskii AI. Significance analysis of spectral count data in label-free shotgun proteomics. Molecular & cellular proteomics: MCP. 2008; 7:2373–2385. [PubMed: 18644780]

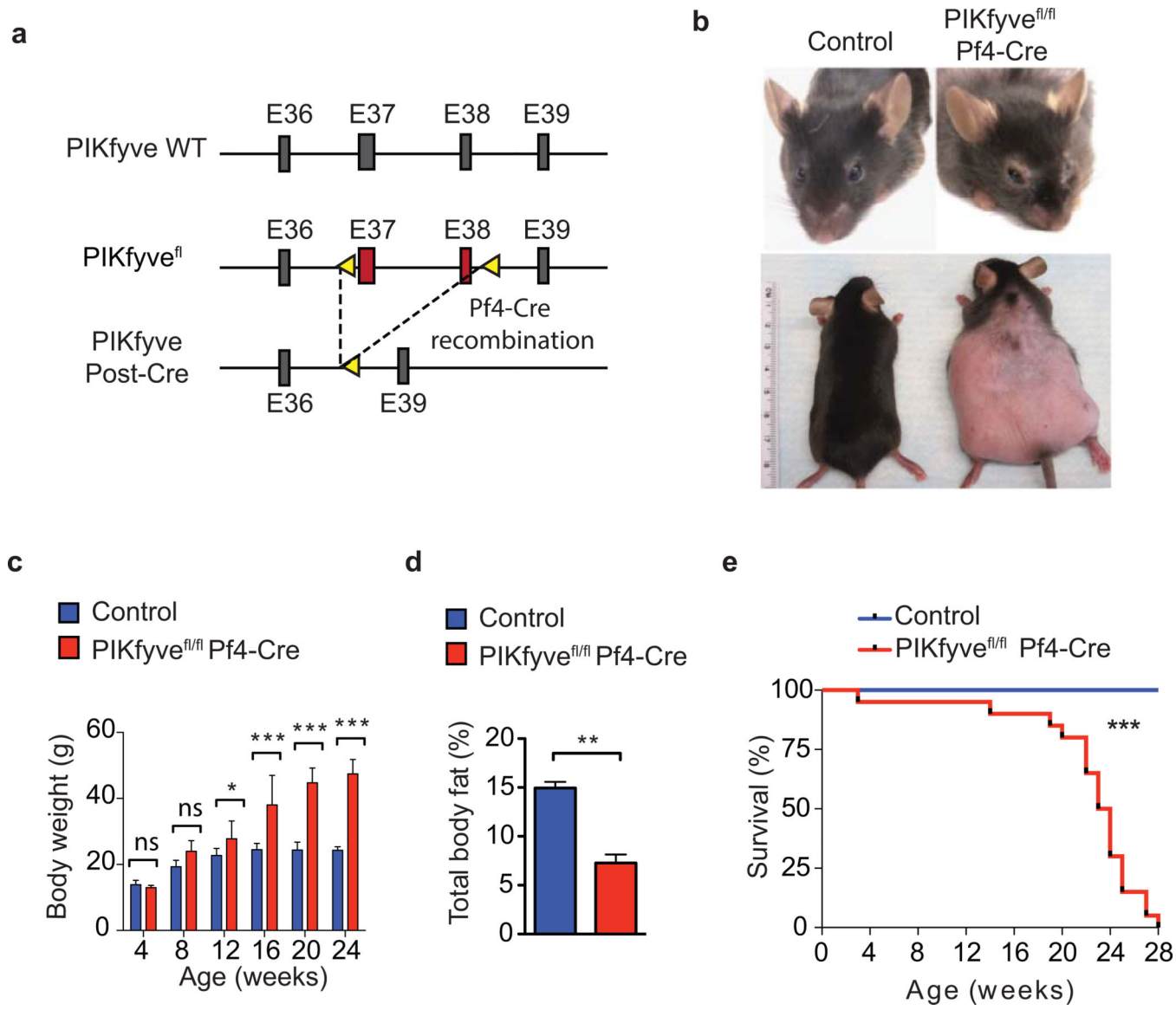

Figure 1. Platelet-specific ablation of PIKfyve causes multiorgan abnormalities in mice

(**a**) Schematic representation of genetic targeting of PIKfyve. The target exons 37and 38 (red bars) were targeted with lox P recombination sites (yellow arrows) to generate PIKfyve floxed alleles (PIKfyve^{fl}). Mice expressing PIKfyve^{fl} were then crossed with Pf4-Cre mice to induce homologous recombination of the PIKfyve^{fl} (PIKfyve Post-Cre). (**b**) General appearance of control and PIKfyve$^{fl/fl}$ Pf4-Cre littermates at 24 weeks of age. Note the characteristic coarse facial features, body hair loss, and severely distended body morphology. (**c**) Body weight of control mice and PIKfyve$^{fl/fl}$ Pf4-Cre mice. The average numbers of mice were 8 per time point and per group. (**d**) Percent of total body fat in the control (n=3) and PIKfyve$^{fl/fl}$ Pf4-Cre (n=3) mice at 12–24 weeks of age. (**e**) Survival curves of control (n= 40) and PIKfyve$^{fl/fl}$ Pf4-Cre (n= 40) mice. *P<0.05, ** P<0.01, ***P<0.001. All error bars indicate mean +/− S.D.

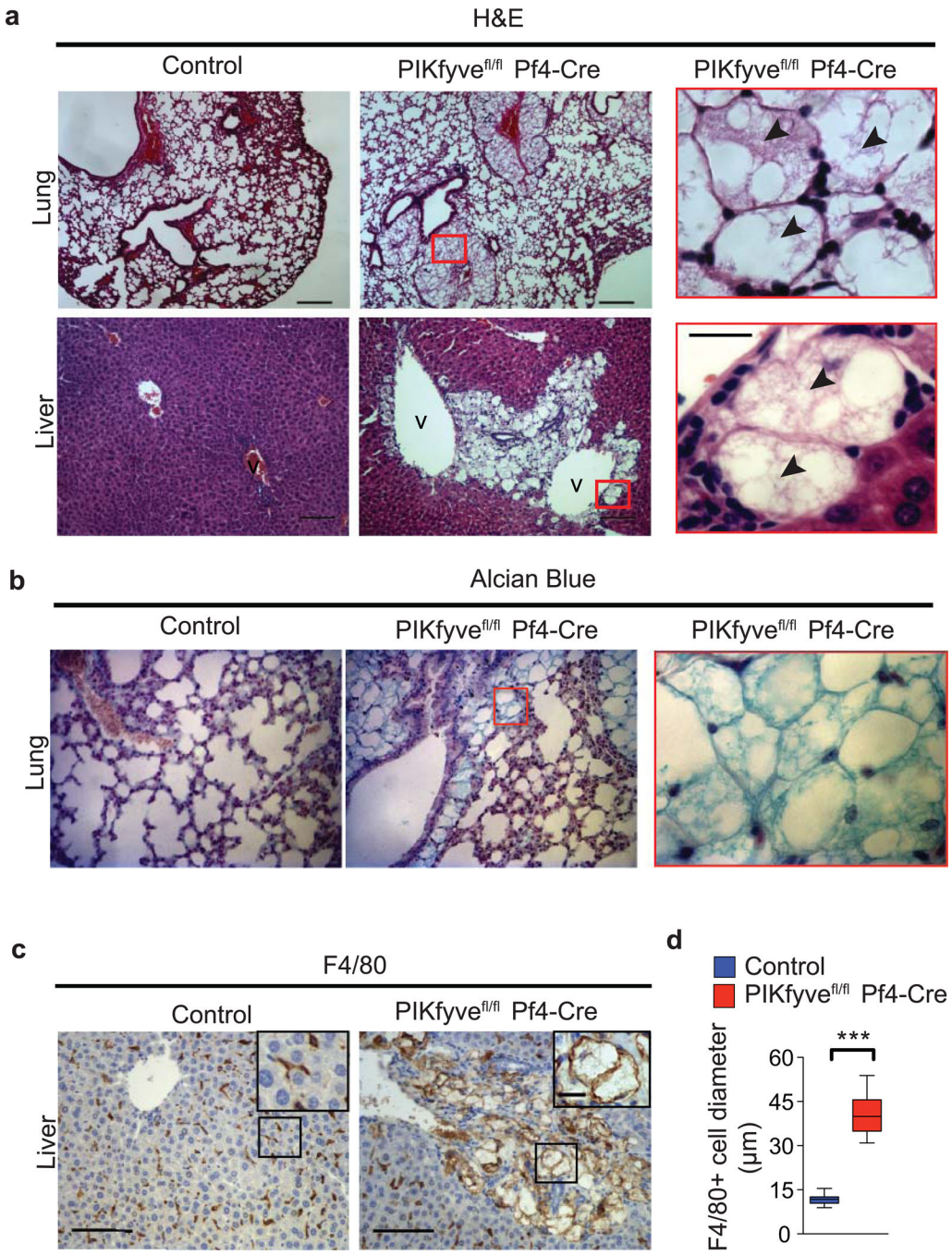

Figure 2. Large vacuolated macrophages infiltrate multiple tissues in the PIKfyve $^{fl/fl}$ Pf4-Cre mice

(**a**) Representative histological sections of the lungs and livers stained with hematoxylin and eosin from control mice and PIKfyve$^{fl/fl}$ Pf4-Cre mice. Scale bar, 100μm. Insets show increased magnification of boxed areas in panel (a). Scale bar, 20μm. Arrowheads indicate the vacuolated cells. (**b**) Lung sections stained with Alcian blue. Scale bar, 100μm. Inset shows high magnification of the boxed area. (**c**) Liver structures of control mice and PIKfyve$^{fl/fl}$ Pf4-Cre mice were stained for macrophages with anti-F4/80 by

immunohistochemistry. Scale bar, 100μm. Insets in the upper right corner of each image show higher magnification images of boxed areas. Scale bar, 20μm. (**d**) Cell diameters of F4/80+ cells in the livers of control mice (n=5) and PIKfyve$^{fl/fl}$ Pf4-Cre mice (n=5). ***P<0.001. All error bars indicate mean +/− S.D.

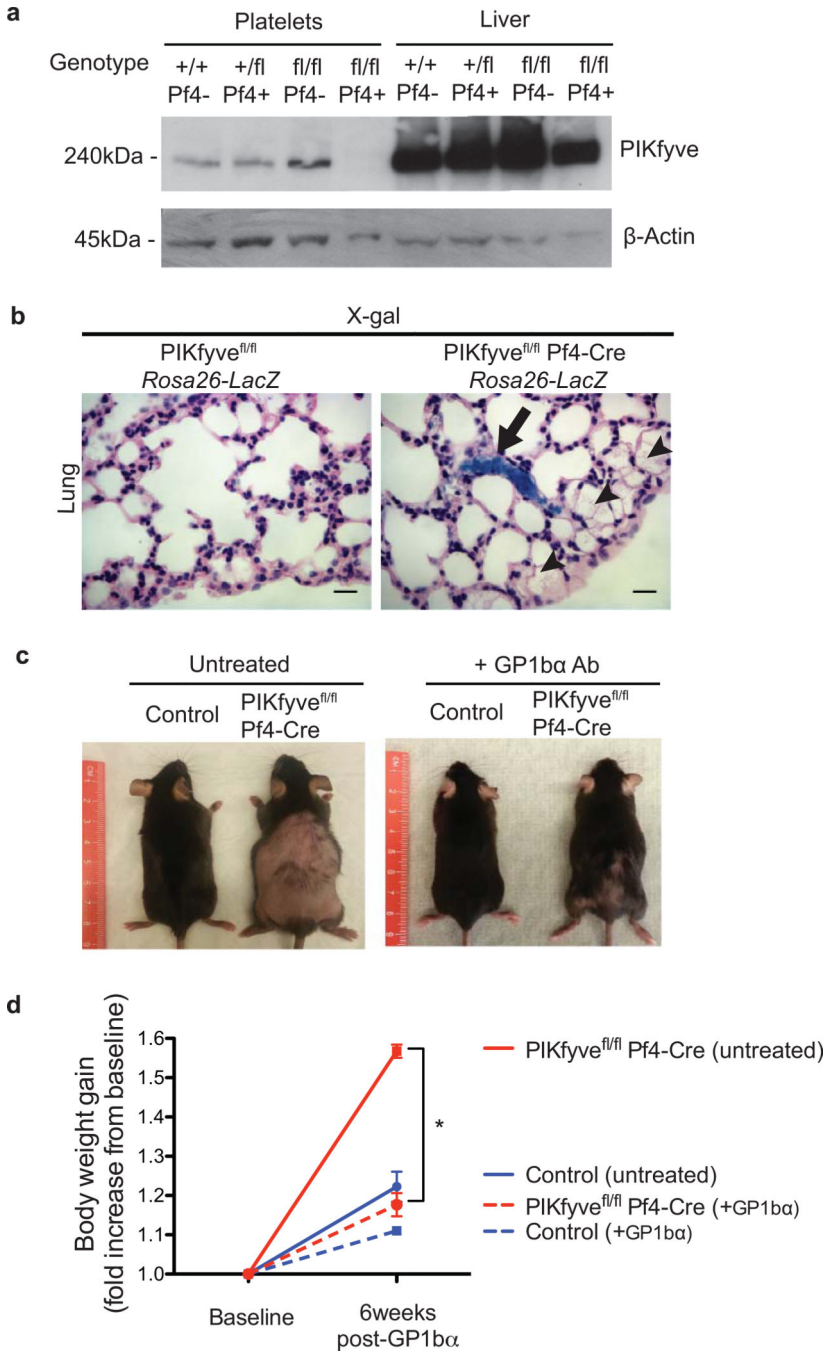

Figure 3. Platelets drive the multiorgan defects in the PIKfyve$^{fl/fl}$ Pf4-Cre mice

(**a**) The levels of PIKfyve protein were determined in the platelets and liver of the indicated mice by immunoblotting. Note the absence of the PIKfyve protein in the platelets, but its presence in the liver of PIKfyve$^{fl/fl}$ Pf4-Cre mice (n=3). Tissues from the wild-type mice, the PIKfyve$^{fl/+}$ Pf4-Cre mice, and the PIKfyve$^{fl/fl}$ mice were used as positive controls. β-actin was used as a loading control. (**b**) X-gal staining of the lung tissues from PIKfyve$^{fl/fl}$ Rosa26-LacZ mice and PIKfyve$^{fl/fl}$ Pf4-Cre Rosa26-LacZ mice. Scale bar, 20μm. The arrow indicates the platelet clumps in the lung vessels expressing LacZ (blue stain). Arrowheads

indicate the vacuolated macrophages that did not stain blue. (**c**) Representative general morphology of 15-weeks-old control mice and PIKfyve$^{fl/fl}$ Pf4-Cre mice after 6 weeks of either no intervention (untreated) or biweekly injections of anti-GP1bα antibodies (+GP1bα Ab). (**d**) Body weight change of the control mice and PIKfyve$^{fl/fl}$ Pf4-Cre mice after 6 weeks of no intervention or treatment with anti-GP1bα antibodies (n=3 for each group). **P*<0.05. All error bars indicate mean +/− S.D.

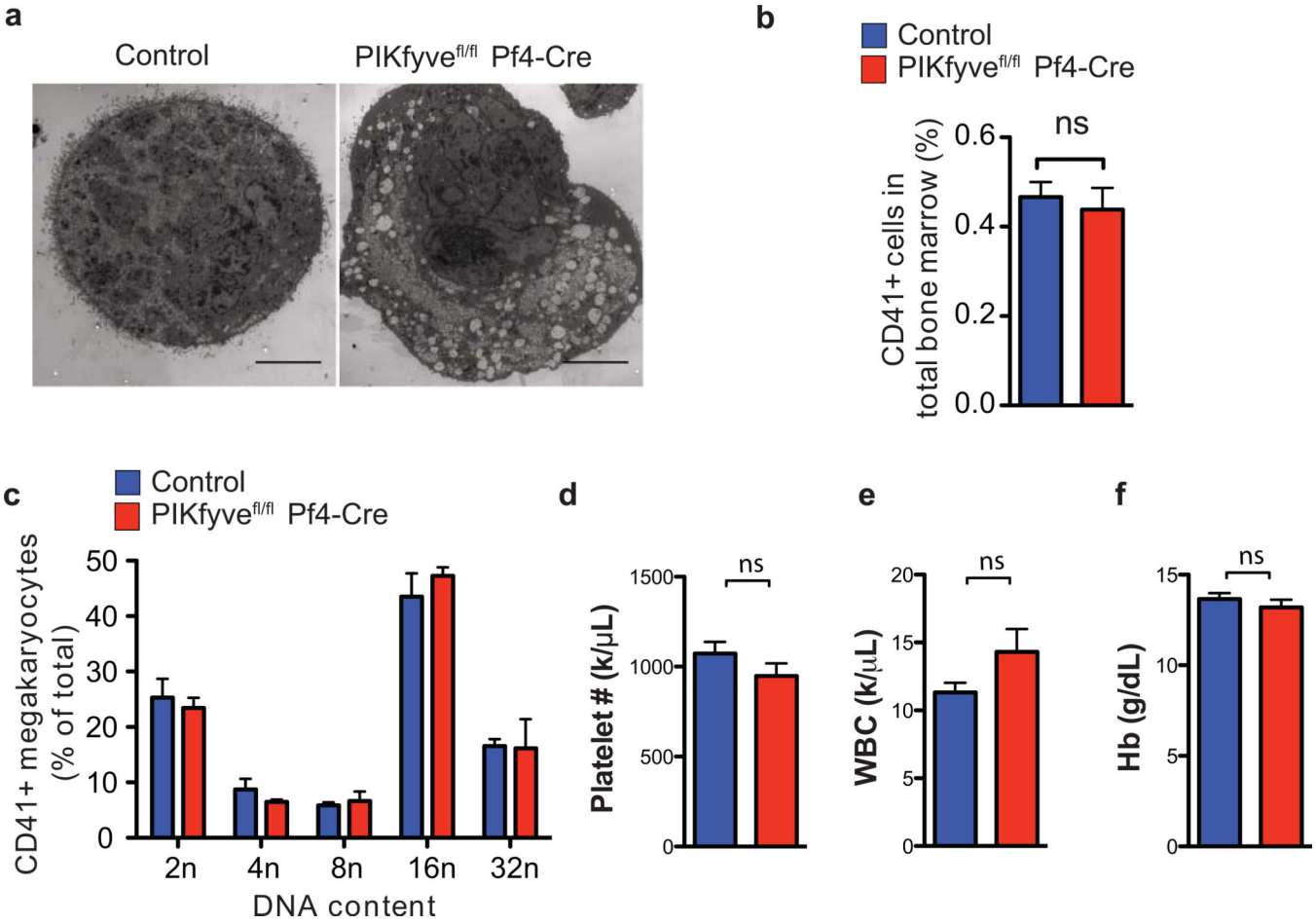

Figure 4. PIKfyve is not necessary for the development of megakaryocytes nor for platelet production

(**a**) Electron micrographs of megakaryocytes grown in culture in the presence of thrombopoietin for 7 days. Note multiple enlarged vacuoles in the cytoplasm of PIKfyve$^{fl/fl}$ Pf4-Cre mice as compared to the control mice. Scale bar, 10μm. (**b**) CD41+ megakaryocyte counts of control PIKfyve$^{fl/fl}$ Pf4-Cre mice. (**c**) Megakaryocyte ploidy. (**d–f**) Counts of platelets (**d**), WBC (**e**), and Hb (**f**) of control mice and PIKfyve$^{fl/fl}$ Pf4-Cre mice.

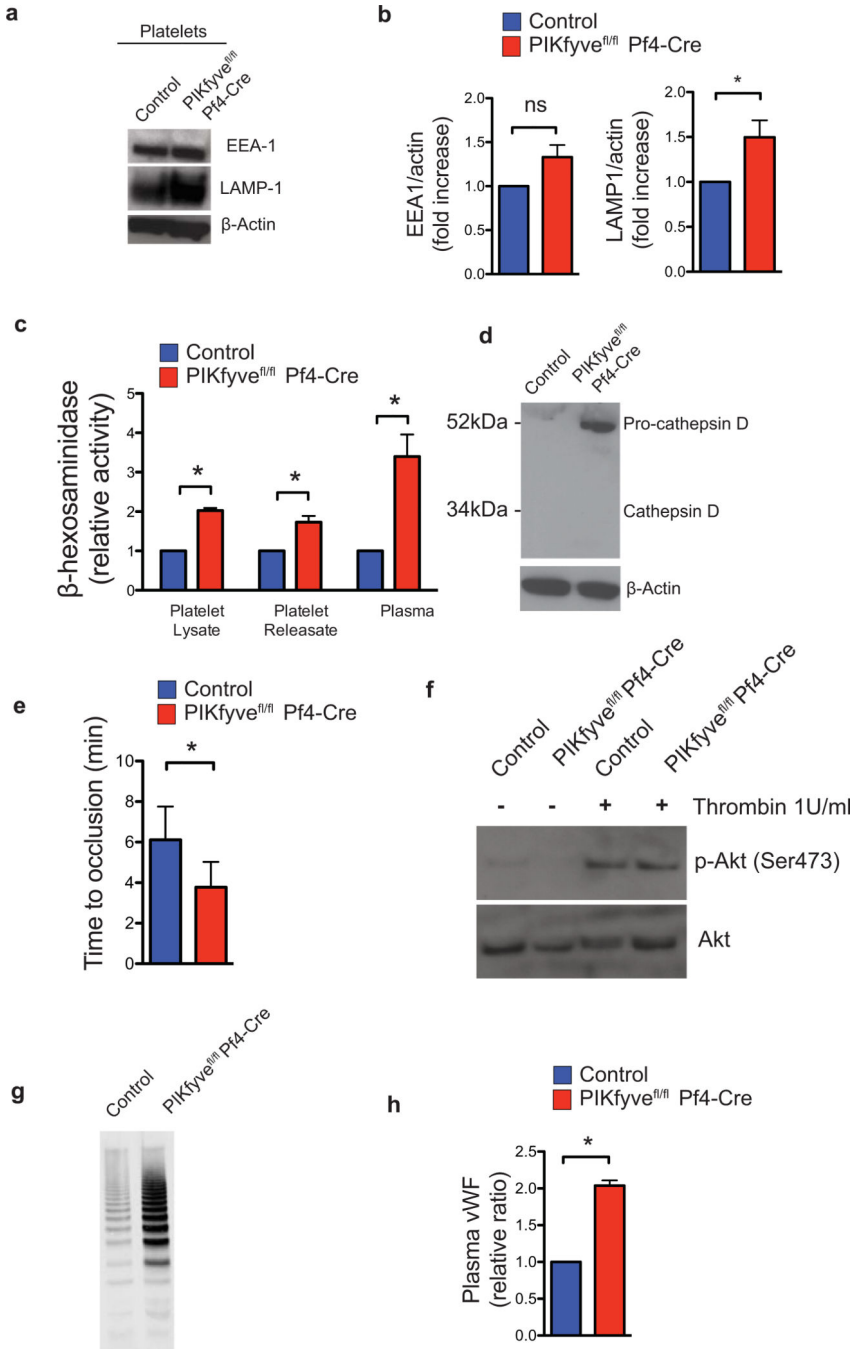

Figure 5. PIKfyve is critical for the maturation, storage, and release of lysosomal enzymes in platelets

(**a**) Immunoblot of platelet lysates from the control mice and PIKfyve$^{fl/fl}$ Pf4-Cre mice showing the expression of EEA-1 and LAMP-1. β-actin was used as the loading control. (**b**) Quantification of protein bands shown in the panel a (n=3 per group). (**c**) β-hexosaminidase activity in the platelet lysates of control mice (n=3) and PIKfyve$^{fl/fl}$ Pf4-Cre mice (n=3). (**d**) β-hexosaminidase activity in the platelet releasate and plasma of control mice (n=3) and PIKfyve$^{fl/fl}$ Pf4-Cre mice (n=3). (**e**) Time to occlusion (TTO) of carotid arteries upon

vascular injury with 7.5% of $FeCl_3$ in the control mice (n=9) and the PIKfyve$^{fl/fl}$ Pf4-Cre mice (n=8). (**f**) Immunoblot of platelet lysates from control platelets and PIKfyve$^{fl/fl}$ Pf4-Cre platelets showing the Akt phosphorylation in resting condition or stimulated with 1U/mL of thrombin for 10 minutes. (**g**) SDS agarose electrophoresis showing the multimer pattern of plasma vWF from the control mice (n=3) and the PIKfyve$^{fl/fl}$ Pf4-Cre (n=3) mice. (**h**) Plasma levels of vWF from the control mice (n=3) and the PIKfyve$^{fl/fl}$ Pf4-Cre (n=3) mice were quantified by ELISA. *P<0.05. All error bars indicate mean +/− S.D.

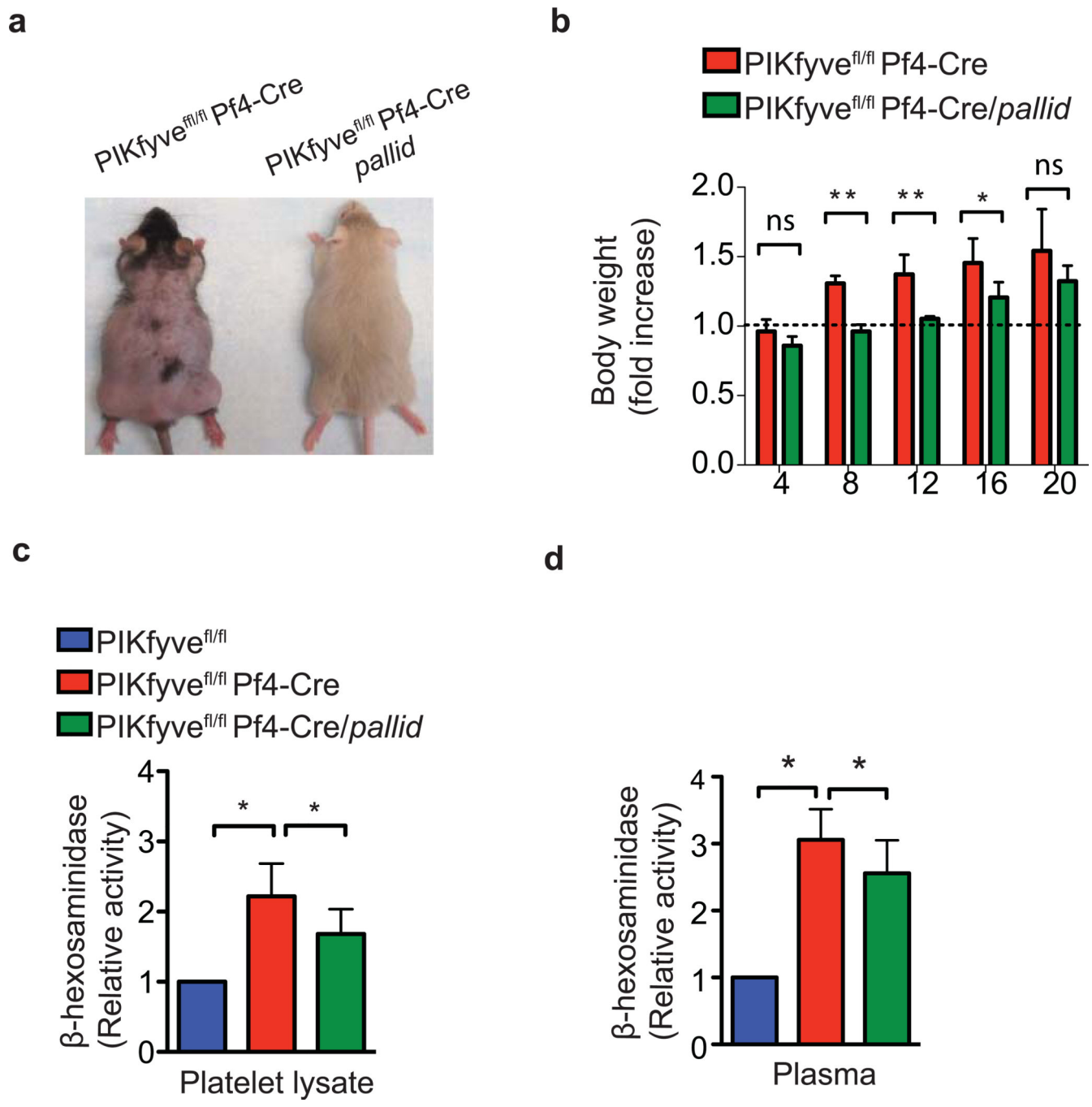

Figure 6. Impaired secretion of platelet lysosomes attenuates the phenotypes of PIKfyve$^{fl/fl}$ Pf4-Cre mice

(**a**) General appearance of PIKfyve$^{fl/fl}$ Pf4-Cre mice and PIKfyve$^{fl/fl}$ Pf4-Cre/*pallid* mice on C57BL/6 background at 17 weeks of age. In the presence of the *pallid* mutation, the hair loss and weight gain are attenuated in the PIKfyve$^{fl/fl}$ Pf4-Cre/*pallid* mice. Note that the *pallid* mice have an underlying defect in melanosome biogenesis causing hypopigmented fur. (**b**) Body weight of the PIKfyve$^{fl/fl}$ Pf4-Cre mice and the aged-matched PIKfyve Pf4-Cre/*pallid* mice. The average numbers of mice were 5 per time point and per group. The

dashed line indicates the mean ratio of body weight of the control mice. (**c,d**) Analysis of β-hexosaminidase activity in the platelet lysate (**c**) and plasma (**d**) of the PIKfyve$^{fl/fl}$ Pf4-Cre mice (n=3) and the PIKfyve$^{fl/fl}$ Pf4-*Cre/pallid* (n=3) mice. **P* <0.05, ** *P* < 0.01. All error bars indicate mean +/− S.D.